

## E(5) Characters to $^{100}\text{Ru}$ Isotope

Sohair M. Diab\* and Salah A. Eid†

\*College of Sciences (Women Section), Phys. Dept., Umm Al-Qura University, Saudi Arabia.

†Faculty of Engineering, Phys. Dept., Ain Shams University, Cairo, Egypt. E-mail: mppe2@yahoo.co.uk

The positive and negative parity states of  $^{100}\text{Ru}$  isotope are studied within the frame work of the interacting boson approximation model ( $IBA - 1$ ). The calculated levels energy, potential energy surfaces,  $V(\beta, \gamma)$ , and the electromagnetic transition probabilities,  $B(E1)$  and  $B(E2)$ , show that  $^{100}\text{Ru}$  isotope has  $E(5)$  Characters. Staggering effect,  $\Delta I = 1$ , has been observed between the positive and negative parity states. The electric monopole strength,  $X(E0/E2)$ , has been calculated. All calculated values are compared to the available experimental, theoretical data and reasonable agreement has been obtained.

### 1 Introduction

The mass region  $A = 100$  has been of considerable interest for nuclear structure studies as it shows many interesting features. These nuclei show back bending at high spin and shape transitions from vibrational to  $\gamma$ -soft and rotational characters. Many attempts have been made to explore these structural changes which is due mainly to the n-p interactions.

Experimentally, the nuclear reaction  $^{100}\text{Mo} (\alpha, xn)$  [1] has been used in studying levels energy of  $^{100}\text{Ru}$ . Angular distribution,  $\gamma$ - $\gamma$  coincidences were measured, half-life time has been calculated and changes to the level scheme were proposed. Also, double beta decay rate of  $^{100}\text{Mo}$  to the first excited  $0^+$  state of  $^{100}\text{Ru}$  has been measured experimentally [2] using  $\gamma$ - $\gamma$  coincidence technique.

Doppler-shift attenuation measurements following the  $^{100}\text{Ru} (n, n'\gamma)$  reaction [3] has been used to measure the life times of the excited states in  $^{100}\text{Ru}$ . Absolute transition rates were extracted and compared with the interacting boson model description. The  $2^+$  (2240.8 keV) state which decays dominantly to the  $2^+$  via 1701 keV transition which is almost pure  $M1$  in nature considered as a mixed-symmetry state. Again  $^{100}\text{Ru}$  has been studied [4] experimentally and several levels were seen where some new ones are detected below 3.2 MeV.

Theoretically many models have been applied to ruthenium isotopes. Yukawa folded mean field [5] has been applied to  $^{100}\text{Ru}$  nucleus while the microscopic vibrational model has been applied to  $^{104}\text{Ru}$  and some other nuclei with their daughters [6]. The latter model was successful in describing the yrast  $0^+$  and  $2^+$  states of most of these nuclei and also some of their half-lives.

The very high-spin states of nuclei near  $A \approx 100$  are investigated by the Cranked Strutinsky method [7] and many very extended shape minima are found in this region. Interacting boson model has been used in studying  $\text{Ru}$  isotopes using a  $U(5)-O(6)$  transitional Hamiltonian with fixed parameters [8-10] except for the boson number  $N$ . Hartree-Fock Bogoliubov [11] wave functions have been tested by comparing the theoretically calculated results for  $^{100}\text{Mo}$  and  $^{100}\text{Ru}$  nuclei with the available experimental data. The yrast spectra,

reduced  $B(E2, 0^+ \rightarrow 2^+)$  transition probabilities, quadrupole moments  $Q(2^+)$  and g factors,  $g(2^+)$  are computed. A reasonable agreement between the calculated and observed values has been obtained.

The microscopic anharmonic vibrator approach (MAVA) [12] has been used in investigating the low-lying collective states in  $^{98-108}\text{Ru}$ . Analysis for the level energies and electric quadrupole decays of the two-phonon type of states indicated that  $^{100}\text{Ru}$  can be interpreted as being a transitional nucleus between the spherical anharmonic vibrator  $^{98}\text{Ru}$  and the quasirotational  $^{102-106}\text{Ru}$  isotopes.

A new empirical approach has been proposed [13] which is based on the connection between transition energies and spin. It allows one to distinguish vibrational from rotational characters in atomic nuclei. The cranked interacting boson model [14] has been used in estimating critical frequencies for the rotation-induced spherical-to-deformed shape transition in  $A = 100$  nuclei. The predictions show an agreement with the back bending frequencies deduced from experimental yrast sequences in these nuclei.

The aim of the present work is to use the  $IBA - 1$  [15, 16] for the following tasks:

1. Calculating the potential energy surfaces,  $V(\beta, \gamma)$ , to know the type of deformation existing for  $^{100}\text{Ru}$ ;
2. Calculating levels energy, electromagnetic transition rates  $B(E1)$  and  $B(E2)$ ;
3. Studying the relation between the angular momentum  $I$  and the rotational angular frequency  $\hbar\omega$  for bending in  $^{100}\text{Ru}$ ;
4. Calculating staggering effect to see beat patterns and detect any interactions between the (+ve) and (-ve) parity states, and
5. Calculating the electric monopole strength  $X(E0/E2)$ .

## 2 (IBA-1) model

### 2.1 Level energies

IBA-1 model was applied to the positive and negative parity states of  $^{100}\text{Ru}$  isotope. The Hamiltonian employed in the

nucleus	<i>EPS</i>	<i>PAIR</i>	<i>ELL</i>	<i>QQ</i>	<i>OCT</i>	<i>HEX</i>	<i>E2SD(eb)</i>	<i>E2DD(eb)</i>
<sup>100</sup> Ru	0.5950	0.000	0.0085	-0.0200	0.0000	0.0000	0.1160	-0.3431

Table 1: Parameters used in IBA-1 Hamiltonian (all in MeV).

present calculation is:

$$H = EPS \cdot n_d + PAIR \cdot (P \cdot P) + \frac{1}{2} ELL \cdot (L \cdot L) + \frac{1}{2} QQ \cdot (Q \cdot Q) + 5OCT \cdot (T_3 \cdot T_3) + 5HEX \cdot (T_4 \cdot T_4) \quad (1)$$

where

$$P \cdot P = \frac{1}{2} \left[ \begin{array}{c} \{(s^\dagger s^\dagger)_0^{(0)} - \sqrt{5}(d^\dagger d^\dagger)_0^{(0)}\} x \\ \{(ss)_0^{(0)} - \sqrt{5}(\tilde{d}\tilde{d})_0^{(0)}\} \end{array} \right]_0^{(0)}, \quad (2)$$

$$L \cdot L = -10\sqrt{3} \left[ (d^\dagger \tilde{d})^{(1)} x (d^\dagger \tilde{d})^{(1)} \right]_0^{(0)}, \quad (3)$$

$$Q \cdot Q = \sqrt{5} \left[ \begin{array}{c} \left\{ (S^\dagger \tilde{d} + d^\dagger s)^{(2)} - \frac{\sqrt{7}}{2} (d^\dagger \tilde{d})^{(2)} \right\} x \\ \left\{ (s^\dagger \tilde{d} + \tilde{d}s)^{(2)} - \frac{\sqrt{7}}{2} (d^\dagger \tilde{d})^{(2)} \right\} \end{array} \right]_0^{(0)}, \quad (4)$$

$$T_3 \cdot T_3 = -\sqrt{7} \left[ (d^\dagger \tilde{d})^{(2)} x (d^\dagger \tilde{d})^{(2)} \right]_0^{(0)}, \quad (5)$$

$$T_4 \cdot T_4 = 3 \left[ (d^\dagger \tilde{d})^{(4)} x (d^\dagger \tilde{d})^{(4)} \right]_0^{(0)}. \quad (6)$$

In the previous formulas,  $n_d$  is the number of boson;  $P \cdot P$ ,  $L \cdot L$ ,  $Q \cdot Q$ ,  $T_3 \cdot T_3$  and  $T_4 \cdot T_4$  represent pairing, angular momentum, quadrupole, octupole and hexadecupole interactions between the bosons; *EPS* is the boson energy; and *PAIR*, *ELL*, *QQ*, *OCT*, *HEX* is the strengths of the pairing, angular momentum, quadrupole, octupole and hexadecupole interactions.

## 2.2 Transition rates

The electric quadrupole transition operator employed in this study is:

$$T^{(E2)} = E2SD \cdot (s^\dagger \tilde{d} + d^\dagger s)^{(2)} + \frac{1}{\sqrt{5}} E2DD \cdot (d^\dagger \tilde{d})^{(2)}. \quad (7)$$

*E2SD* and *E2DD* are adjustable parameters.

The reduced electric quadrupole transition rates between  $I_i \rightarrow I_f$  states are given by:

$$B(E2, I_i \rightarrow I_f) = \frac{[ \langle I_f || T^{(E2)} || I_i \rangle ]^2}{2I_i + 1}. \quad (8)$$

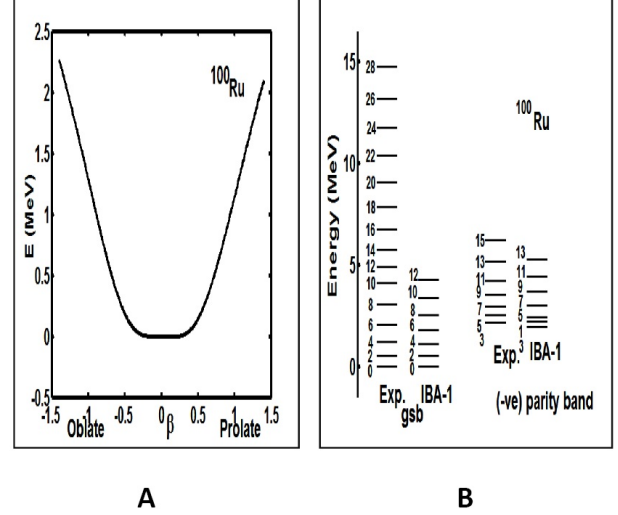


Fig. 1: A: Potential energy surfaces for <sup>100</sup>Ru. B: Comparison between exp. [19] and theoretical IBA-1 energy levels.

## 3 Results and discussion

### 3.1 The potential energy surfaces

The potential energy surfaces [17],  $V(\beta, \gamma)$ , as a function of the deformation parameters  $\beta$  and  $\gamma$  are calculated using:

$$E_{N_\pi N_\nu}(\beta, \gamma) = \langle N_\pi N_\nu; \beta \gamma | H_{\pi\nu} | N_\pi N_\nu; \beta \gamma \rangle = \zeta_d(N_\nu N_\pi) \beta^2 (1 + \beta^2) + \beta^2 (1 + \beta^2)^{-2} \times \left\{ k N_\nu N_\pi [4 - (\bar{X}_\pi \bar{X}_\nu) \beta \cos 3\gamma] + \left[ \bar{X}_\pi \bar{X}_\nu \beta^2 + N_\nu (N_\nu - 1) \left( \frac{1}{10} c_0 + \frac{1}{7} c_2 \right) \beta^2 \right] \right\}, \quad (9)$$

where

$$\bar{X}_\rho = \left( \frac{2}{7} \right)^{0.5} X_\rho \quad \rho = \pi \text{ or } \nu. \quad (10)$$

The calculated potential energy surfaces,  $V(\beta, \gamma)$ , are presented in Fig. 1A. The flat potential in the critical symmetry point has supported quite well the *E(5)* characters to <sup>100</sup>Ru nucleus. Also, the energy ratios presented in Table 4 as well as the existence of <sup>100</sup>Ru isotope between the spherical anharmonic vibrator <sup>98</sup>Ru and  $\gamma$ -soft <sup>102</sup>Ru nuclei [9] supported the *E(5)* characters.

### 3.2 Energy spectra

The energy of the positive and negative parity states of <sup>100</sup>Ru isotope are calculated using computer code PHINT [18]. A

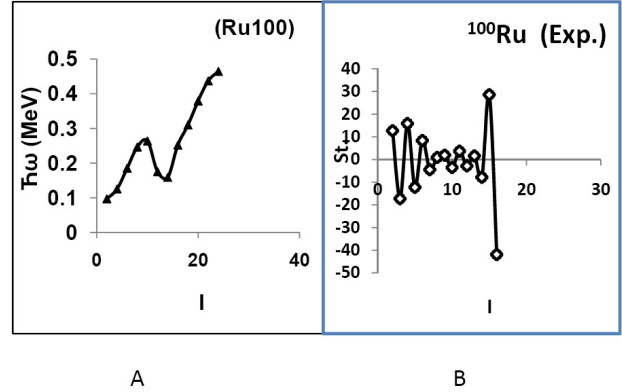
$I_i^+ I_f^+$	B(E2)	$I_i^+ I_f^+$	B(E1)
0 <sub>1</sub> Exp*. 2 <sub>1</sub>	0.490(5)	1 <sub>1</sub> 0 <sub>1</sub>	0.0030
0 <sub>1</sub> Theor. 2 <sub>1</sub>	0.4853	1 <sub>1</sub> 0 <sub>2</sub>	0.1280
2 <sub>1</sub> 0 <sub>1</sub>	0.0970	3 <sub>1</sub> 2 <sub>1</sub>	0.1211
2 <sub>2</sub> 0 <sub>1</sub>	0.0006	3 <sub>1</sub> 2 <sub>2</sub>	0.0415
2 <sub>2</sub> 0 <sub>2</sub>	0.0405	3 <sub>1</sub> 2 <sub>3</sub>	0.0002
2 <sub>3</sub> 0 <sub>1</sub>	0.0000	3 <sub>2</sub> 2 <sub>1</sub>	0.0024
2 <sub>3</sub> 0 <sub>2</sub>	0.0759	3 <sub>2</sub> 2 <sub>2</sub>	0.0197
2 <sub>3</sub> 0 <sub>3</sub>	0.0087	3 <sub>2</sub> 2 <sub>3</sub>	0.2126
2 <sub>4</sub> 0 <sub>3</sub>	0.0066	5 <sub>1</sub> 4 <sub>1</sub>	0.2533
2 <sub>4</sub> 0 <sub>4</sub>	0.0588	5 <sub>1</sub> 4 <sub>2</sub>	0.0480
4 <sub>1</sub> 2 <sub>1</sub>	0.1683	5 <sub>1</sub> 4 <sub>3</sub>	0.0006
4 <sub>1</sub> 2 <sub>2</sub>	0.0142	7 <sub>1</sub> 6 <sub>1</sub>	0.3950
4 <sub>1</sub> 2 <sub>3</sub>	0.0319	7 <sub>1</sub> 6 <sub>2</sub>	0.0446
6 <sub>1</sub> 4 <sub>1</sub>	0.2039	9 <sub>1</sub> 8 <sub>1</sub>	0.5439
6 <sub>1</sub> 4 <sub>2</sub>	0.0179	9 <sub>1</sub> 8 <sub>2</sub>	0.0342
6 <sub>1</sub> 4 <sub>3</sub>	0.0242	11 <sub>1</sub> 10 <sub>1</sub>	0.6983
8 <sub>1</sub> 6 <sub>1</sub>	0.2032		
8 <sub>1</sub> 6 <sub>2</sub>	0.0183		
8 <sub>1</sub> 6 <sub>3</sub>	0.0157		
10 <sub>1</sub> 8 <sub>1</sub>	0.1678		
10 <sub>1</sub> 8 <sub>2</sub>	0.0175		

Table 2: Calculated  $B(E2)$  and  $B(E1)$  in  $^{100}\text{Ru}$ .

$I_i^+$	$I_f^+$	$I_f^+$	$X_{if'f}(E0/E2)^{100}\text{Ru}$
0 <sub>2</sub>	0 <sub>1</sub>	2 <sub>1</sub>	0.027
0 <sub>3</sub>	0 <sub>1</sub>	2 <sub>1</sub>	0.347
0 <sub>3</sub>	0 <sub>1</sub>	2 <sub>2</sub>	0.009
0 <sub>3</sub>	0 <sub>1</sub>	2 <sub>3</sub>	0.042
0 <sub>3</sub>	0 <sub>2</sub>	2 <sub>1</sub>	0.086
0 <sub>3</sub>	0 <sub>2</sub>	2 <sub>2</sub>	0.002
0 <sub>3</sub>	0 <sub>2</sub>	2 <sub>3</sub>	0.010
0 <sub>4</sub>	0 <sub>1</sub>	2 <sub>2</sub>	0.010
0 <sub>4</sub>	0 <sub>1</sub>	2 <sub>3</sub>	0.010
0 <sub>4</sub>	0 <sub>1</sub>	2 <sub>4</sub>	0.113
0 <sub>4</sub>	0 <sub>2</sub>	2 <sub>2</sub>	0.030
0 <sub>4</sub>	0 <sub>2</sub>	2 <sub>3</sub>	0.034
0 <sub>4</sub>	0 <sub>2</sub>	2 <sub>4</sub>	0.340
0 <sub>4</sub>	0 <sub>3</sub>	2 <sub>1</sub>	0.454
0 <sub>4</sub>	0 <sub>3</sub>	2 <sub>2</sub>	0.010
0 <sub>4</sub>	0 <sub>3</sub>	2 <sub>3</sub>	0.011
0 <sub>4</sub>	0 <sub>3</sub>	2 <sub>4</sub>	0.113

Table 3: Calculated  $X_{if'f}(E0/E2)$ .

Energy Ratios	$E_{4^+}/E_{2^+}$	$E_{2^+}/E_{2^+}$
$E(5)$	2.19	2.20
Exp. [19]	2.27	2.52
$IBA - 1$	2.12	2.11

Table 4: Energy ratios of  $E(5)$  characters to  $^{100}\text{Ru}$ .Fig. 2: A: Angular momentum  $I$  as a function of  $(\hbar\omega)$ . B:  $(\Delta I = 1)$ , staggering pattern for  $^{100}\text{Ru}$  isotope.

comparison between the experimental spectra [19] and our calculations, using values of the model parameters given in Table 1 for the ground state band are illustrated in Fig. 1B. The agreement between the calculated levels energy and their correspondence experimental values are slightly higher especially for the higher excited states. We believe this is due to the change of the projection of the angular momentum which is due mainly to band crossing.

Unfortunately there is not enough measurements of electromagnetic transition rates  $B(E1)$  or  $B(E2)$  for  $^{100}\text{Ru}$  nucleus. The only measured  $B(E2, 0_1^+ \rightarrow 2_1^+)$  is presented, in Table 2 for comparison with the calculated values [20]. The parameters  $E2SD$  and  $E2DD$  displayed in Table 1 are used in the computer code NPBEM [18] for calculating the electromagnetic transition rates after normalized to the available experimental values. No new parameters are introduced for calculating electromagnetic transition rates  $B(E1)$  and  $B(E2)$  of intraband and interband.

The moment of inertia  $I$  and angular frequency  $\hbar\omega$  are calculated using equations (11, 12):

$$\frac{2I}{\hbar^2} = \frac{4I - 2}{\Delta E(I \rightarrow I - 2)}, \quad (11)$$

$$(\hbar\omega)^2 = (I^2 - I + 1) \left[ \frac{\Delta E(I \rightarrow I - 2)}{(2I - 1)} \right]^2. \quad (12)$$

The plot in Fig. 2A show back bending at angular momentum  $I^+ = 10$ . It means, there is a crossing between the  $(+ve)$  and  $(-ve)$  parity states in the ground state band which

was confirmed by calculating the staggering effect where a beat pattern has been observed, Fig. 2B.

### 3.3 Electric monopole transitions

The electric monopole transitions,  $E0$ , are normally occurring between two states of the same spin and parity by transferring energy and zero unit of angular momentum. The strength of the electric monopole transition,  $X_{if'f}(E0/E2)$ , [21] can be calculated using equations (13, 14); results are presented in Table 3

$$X_{if'f}(E0/E2) = \frac{B(E0, I_i - I_f)}{B(E2, I_i - I_f)}, \quad (13)$$

$$X_{if'f}(E0/E2) = (2.54 \times 10^9) A^{3/4} \times \frac{E_\gamma^5(\text{MeV})}{\Omega_{KL}} \alpha(E2) \frac{T_e(E0, I_i - I_f)}{T_e(E2, I_i - I_f)}. \quad (14)$$

Here:  $A$  is mass number;  $I_i$  is spin of the initial state where  $E0$  and  $E2$  transitions are depopulating it;  $I_f$  is spin of the final state of  $E0$  transition;  $I_f$  is spin of the final state of  $E2$  transition;  $E_\gamma$  is gamma ray energy;  $\Omega_{KL}$  is electronic factor for K,L shells [22];  $\alpha(E2)$  is conversion coefficient of the  $E2$  transition;  $T_e(E0, I_i - I_f)$  is absolute transition probability of the  $E0$  transition between  $I_i$  and  $I_f$  states, and  $T_e(E2, I_i - I_f)$  is absolute transition probability of the  $E2$  transition between  $I_i$  and  $I_f$  states.

### 3.4 The staggering

The presence of  $(+ve)$  and  $(-ve)$  parity states has encouraged us to study staggering effect [23–25] for  $^{100}\text{Ru}$  isotope using staggering function equations (15, 16) with the help of the available experimental data [19].

$$St(I) = 6\Delta E(I) - 4\Delta E(I-1) - 4\Delta E(I+1) + \Delta E(I+2) + \Delta E(I-2), \quad (15)$$

with

$$\Delta E(I) = E(I+1) - E(I). \quad (16)$$

The calculated staggering patterns are illustrated in Fig. 2B and show an interaction between the  $(+ve)$  and  $(-ve)$  parity states for the ground state band of  $^{100}\text{Ru}$ .

### 3.5 Conclusions

IBA-1 model has been applied successfully to  $^{100}\text{Ru}$  isotope and:

1. The levels energy are successfully reproduced;
2. The potential energy surfaces are calculated and show  $E(5)$  Characters to  $^{100}\text{Ru}$ ;
3. Electromagnetic transition rates  $B(E1)$  and  $B(E2)$  are calculated;
4. Bending for  $^{100}\text{Ru}$  has been observed at angular momentum  $I^+ = 10$ ;

5. Strength of the electric monopole transitions  $X_{if'f}(E0/E2)$  are calculated; and
6. Staggering effect has been calculated and beat pattern has been obtained, showing an interaction between the  $(-ve)$  and  $(+ve)$  parity states.

Submitted on: December 12, 2012 / Accepted on: December 20, 2012

### References

1. Maazek J., Honusek M., Spalek A., Bielik J., Slivova J. and Pasternak A. A. Levels of  $^{100,101}\text{Ru}$  excited in the reaction  $^{100}\text{Mo}(\alpha\chi n)$ . *Acta Physica Polonica B*, 1998, v. 29, 433.
2. Braeckeleer L. L., Hornish M., Barabash A. and Umatov V. Measurement of the  $\beta\beta$ -decay rate of  $^{100}\text{Mo}$  to the first excited  $0^+$  state of  $^{100}\text{Ru}$ . *Physical Review*, 2001, v. 86, 3510.
3. Genilloud L., Brown T. B., Corminboeuf F., Garrett P. E., Hannant C. D., Jolie J., Warr N. and Yates S. W. Characterization of the three-phonon region of  $^{100}\text{Ru}$ . *Nuclear Physics A*, 2001, v. 683, 287.
4. Horodyski-Matsushigue L. H., Rodrigues C. L., Sampaio F. C. and Lewin T. B. Particle spectroscopy of low-lying collective states in  $^{100}\text{Ru}$ . *Nuclear Physics A*, 2002, v. 709, 73.
5. Nerlo-Pomorska B., Pomorski K. and Bartel J. Shell energy and the level-density parameter of hot nuclei. *Physical Review C*, 2006, v. 74, 034327.
6. Raina P. K. and Dhiman R. K. Systematics of  $\beta\beta$  decay sensitive medium mass nuclei using quadrupole-quadrupole plus pairing interactions. *Physical Review C*, 2001, v. 64, 024310.
7. Chasman R. R. Very extended nuclear shapes near  $A = 100$ . *Physical Review C*, 2001, v. 64, 024311.
8. Frank A., Alonso C. E. and Arias J. M. Search for  $E(5)$  symmetry in nuclei: the  $\text{Ru}$  isotopes. *Physical Review C*, 2001, v. 65, 014301.
9. Diab S. M., Eid S. A. Nature of the excited states of the even-even  $^{98-108}\text{Ru}$  isotopes. *Progress in Physics*, 2008, v. 4, 51.
10. Cejnar P., Jolie J. and Kern J. Universal anharmonicity anomaly in nuclei. *Physical Review C*, 2001, v. 63, 047304.
11. Chaturvedi K., Dixit B. M. and Rath P. K. Two neutrino double  $\beta$  decay of  $^{100}\text{Mo}$  to the  $2^+$  excited state of  $^{100}\text{Ru}$ . *Physical Review C*, 2003, v. 67, 064317.
12. Kotila J., Suhonen J. and Delion D. S. Low-lying collective states in  $^{98,106}\text{Ru}$  isotopes studied using a microscopic anharmonic vibrator approach. *Physical Review C*, 2003, v. 68, 054322.
13. Regan P. H., Beausang C. W., Zamfir N. V., Casten R. F., Zhang J., Meyer D. A. and Ressler J. J. Signature for vibrational to rotational evolution along the yrast line. *Physical Review Letters*, 2003, v. 90, 152502.
14. Cejnar P. and Jolie J. Rotation-driven spherical-to-deformed shape transition in  $A \approx 100$  nuclei and the cranked interacting boson model. *Physical Review C*, 2004, v. 69, 011301.
15. Arima A. and Iachello F. Interacting boson model of collective states: The vibrational limit. *Annals of Physics (N.Y.)*, 1976, v. 99, 253.
16. Arima A. and Iachello F. Interacting boson model of collective states: The rotational limit. *Annals of Physics (N.Y.)*, 1978, v. 111, 201.
17. Ginocchio J. N. and Kirson M. W. An intrinsic state for the interacting boson model and its relationship to the Bohr-Mottelson approximation. *Nuclear Physics A*, 1980, v. 350, 31.
18. Scholten O. *The program package PHINT (1980) version, internal report KVI-63, Gronigen: Keryfysisch Versneller Instituut*.
19. Balraj Singh. Adopted levels, gammas for  $^{100}\text{Ru}$ . *Nuclear Data Sheets*, 1997, v. 81, 1997.

20. Raman S., Nestor JR.C.W., and Tikkanen P., Transition probability from the ground to the first-excited  $2^+$  state of even-even nuclides. *Atomic Data and Nuclear Data Tables*, 2001, v. 78, 1.
  21. Rasmussen J. O. Theory of  $E0$  transitions of spheroidal nuclei. *Nuclear Physics*, 1960, v. 19, 85.
  22. Bell A. D., Avelo C. E., Davidson M. G. and Davidson J. P., Table of  $E0$  conversion probability electronic factors. *Canadian Journal of Physics*, 1970, v. 48, 2542.
  23. Minkov N., Yotov P., Drenska S. and Scheid W. Parity shift and beat staggering structure of octupole bands in a collective model for quadrupole-octupole deformed nuclei. *Journal of Physics G*, 2006, v. 32, 497.
  24. Bonatsos D., Daskaloyannis C., Drenska S. B., Karoussos N., Minkov N., Raychev P. P. and Roussev R. P.  $\Delta I = 1$  staggering in octupole bands of light actinides Beat patterns. *Physical Review C*, 2000, v. 62, 024301.
  25. Minkov N., Drenska S. B., Raychev P. P., Roussev R. P. and Bonatsos D. Beat patterns for the odd-even staggering in octupole bands from quadrupole-octupole Hamiltonian. *Physical Review C*, 2001, v. 63, 044305.
-